



Keldysh Institute • Publication search

Keldysh Institute preprints • Preprint No. 29, 2014



Khilkov S. A., Ivanov A. V.

Numerical simulation of the
magnetic moment distribution
evolution for
superparamagnetic materials

Recommended form of bibliographic references: Khilkov S. A., Ivanov A. V. Numerical simulation of the magnetic moment distribution evolution for superparamagnetic materials // Keldysh Institute Preprints. 2014. No. 29. 16 p. URL: <http://library.keldysh.ru/preprint.asp?id=2014-29&lg=e>

Ордена Ленина
ИНСТИТУТ ПРИКЛАДНОЙ МАТЕМАТИКИ
имени М. В. Келдыша
Российской академии наук

S.A. Khilkov, A.V. Ivanov

**Numerical simulation of the magnetic
moment distribution evolution
for superparamagnetic materials**

Москва
2014

Sergey A. Khilkov, Anton V. Ivanov

Numerical simulation of the magnetic moment distribution evolution for superparamagnetic materials

We present in this paper the high-order local discontinuous Galerkin method for solution to Fokker–Planck like equation for superparamagnetics on a sphere. We used the recursively constructed mesh on the sphere which consists of spherical triangles. In addition we provide the ordering of cells which increases the locality of data corresponding to mesh cells. Several test calculations were carried out. They proved the second order of the scheme. In addition, resonant properties of the system for two different setups were calculated.

Keywords: LDG, superparamagnetic, Brown equation

Хилков С.А., Иванов А.В.

Численное моделирование эволюции функции распределения магнитного момента для суперпарамагнитных материалов

В данной работе построен локальный разрывный метод Галеркина высокого порядка для решения уравнения типа Фоккера–Планка для суперпарамагнетиков на сфере. В работе использовалась рекурсивная сетка, состоящая из сферических треугольников, обеспечивающая хорошую локальность хранимых в ней данных. Было проведено несколько тестовых расчетов, подтвердивших второй порядок точности метода. В качестве примера применения метода были рассчитаны резонансные свойства суперпарамагнетика для двух различных постановок.

Ключевые слова: локальный метод Галеркина, суперпарамагнетики, уравнение Брауна.

The work was supported by RFBR grants 12-02-00528a, 12-01-00708-a and 14-01-00787.

Содержание

Introduction	3
1 The mesh and the basis	4
2 The setting of the problem	8
3 The numerical method	9
4 The results of the simulations	12
Concluding remarks	14

Introduction

Solving the equations of physical kinetic on a sphere is required in a wide range of problems. In many settings (especially in evolutionary problems) to obtain an appropriate solution one should use methods which ensure that the conservation laws inherent for a system are fulfilled. Apart from that, many problems require high accuracy. High-order methods are commonly used to increase accuracy without sufficient rise of the computational cost.

To fulfill these demands it is convenient to utilize the results from computational fluid dynamics. Discontinuous Galerkin methods (DG) [1] are the newest and the most promising computational methods family. These methods are straightforwardly generalized to any necessary order of convergence and they possess conservative properties. Also in the recent years the adaptive modifications of the DG methods were developed [2]. The former monotonize the generic limiters [3] along with the limiters designed for a specific problem [4].

Although the DG methods restrict the choice of meshes only to a minor extent, the accuracy of the solution certainly depends on the quality of the mesh. In many problems the errors caused by the mesh anisotropy lead not only to the quantitative distortions but also to the qualitative ones. The traditional mesh in the spherical coordinates is the simplest for implementation, but the singularities on the poles appear to be considerable restrictions in its application. The other approach is called cubed sphere [5] which is constructed by means of projection of a circumscribed cube on a sphere and subsequent decomposition of each quadrangle. This mesh is evidently anisotropic and possesses considerable distortions in the vicinity of the corner of the cube, although it already is viable. There exists a plenty of other choices of the meshes on the sphere, see for example a mesh based on an icosahedron in the work by Giraldo [6]. We implement a recursive mesh based on a dodecahedron [7]. The basic mesh is obtained after the primary decomposition of its faces to almost equilateral triangles. The subsequent splitting of the triangles and projection to the sphere provides considerably less distortion than the mesh based on an icosahedron. To approbate this method we simulate a superparamagnetic, which is an ensemble of monodomain ferromagnetic microparticles. The superparamagnetics are described by an equation of the Fokker–Planck type on a sphere, derived by Brown in 1963 [8]. It is among the simplest equations of the physical kinetic considered on a sphere. For some particular cases a precise analytical solution to the Brown equation is available and allows us to test the method. Apart from that the superparamagnetics possess a number of

interesting resonant properties. In this work we calculated the response dependence on the temperature for two qualitatively different cases, in both apart from the paramagnetic resonance nonmonotonic dependence of the response on the temperature (stochastic resonance) could be observed.

The paper describes a local discontinuous Galerkin method (LDG) for the numerical solution of the Brown equation on a sphere. For a number of simplifications the comparison to the precise solutions are provided. The first Section defines the mesh and the basis in cells, the second Section describes mathematical and physical setting, the third Section defines the numerical method and in the last Section the results of the calculations are presented.

1 The mesh and the basis

1.1 The mesh

The implementation of the DG method admits meshes of quite a generic type, for example in the work by Giraldo [6] the mesh consisting of curved quadrangles is used. We use the tessellation $\mathcal{T}_h = \{K_i, i = \overline{1, n}\}$ on a spherical region S^2 which consists of N spherical triangles K_i . While simulating the precession of the distribution one has to take into account the curvature of the cells because on the mesh of plane triangles a systematic phase error inevitably appears.

The construction of the mesh on a sphere is a separate complicated task. We have decided to use a recursive algorithm of construction. One of its advantages is a relative simplicity of local mesh refinement and consequently the simplicity of the development of the adaptive methods. It is worth mentioning that the discontinuous Galerkin method also allows to tune the order of accuracy in a separate cell without splitting of the cells using the enlargement of the basis in a given cell of the numerical scheme. Another advantage of recursive mesh structure is a natural locality of the data. Also it is convenient that the discussed mesh possesses a large number of symmetries. This property is used in particular to decrease the amount of the geometric data stored and calculated.

The construction of the mesh was started from a dodecahedron in which the vertices of a given face are connected with the center of the face. The starting mesh is obtained by a projection of this polyhedron to the sphere. To simplify the calculations one can rotate the dodecahedron in such a way that any of the coordinate planes would contain a pair of the opposite edges of the dodecahedron. Such an orientation on the space allows to reduce the main

part of the symmetries to the cyclic permutations of the coordinates and to the reflections from the coordinate planes. Thus there remain only two unique vertices of the dodecahedron. The decomposition of the triangle is carried out by the connection of the centers of its edges (cf. fig. 3). An example of a tessellation on the sphere is given on the fig. 1.

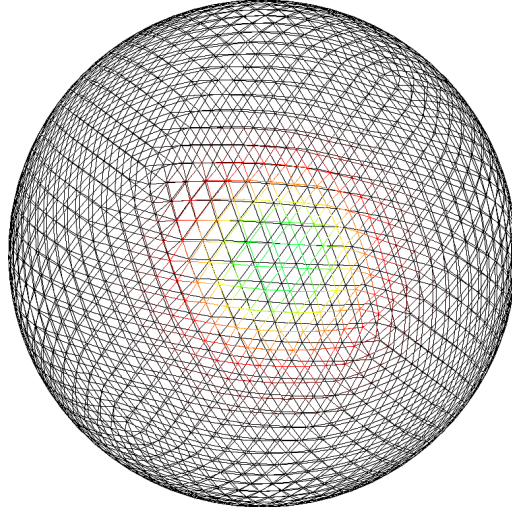


Figure 1: The mesh after three steps of the decomposition of the triangles.

For the mesh calculations it is important to know how the linear size of the cell decreases when the number of cells increases. From the fig. 2 one can see that the linear size is proportional to a square root of the number of cells which is natural in two-dimensional problems.

For the effective realization of the calculation the locality of the data (i.e. how closely the neighbouring cells are located in the memory) is rather important [9]. To obtain a mesh with high locality we utilize the following indexation algorithm. All the data are stored in a one-dimensional array. The index of a given cell in this array is constructed recursively. Any of the pentagons of the dodecahedron is located in two quadrants, and this pair of quadrants defines it unambiguously. The indices of the triangles increase clockwise and are ordered by the indices of pentagons which contain them. In any subsequent level of decomposition the index of triangles are ordered by entering of the triangle in the previous triangle (sf. fig. 3). Inside the triangle the indices increase clockwise and the minimal index is in the center. Thus if we write index for triangle K_i in quaternary notation we see that first two digits represent index for triangle of mesh without decomposition, which contain K_i , first three digits form the index on the mesh after one step of triangles decomposition and so on. On each step of decomposition we add one new digit in the end of index.

Such an ordering increases the locality of the data. Also linking the internal

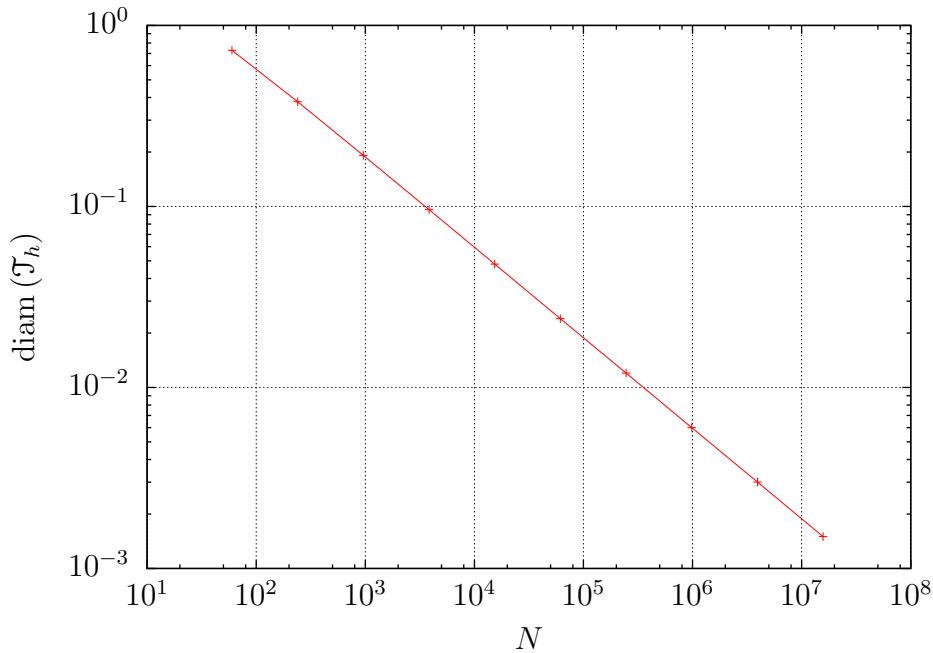


Figure 2: The dependence of the diameter of the tessellation $\text{diam}(\mathcal{T}_h)$ on the number of the cells N .

ordering allows to construct a simple algorithm of search of neighbouring cells based on the index of the given cell which does not require any additional data.

1.2 The basis

Let us start with writing down the basis in the triangle K_i . We construct the basis from the spherical Bernstein–Bezier polynomials [10]. In principle it is straightforward to write the basis for any given order of accuracy, but in this paper we confine ourselves to the second order. For the second-order method the basis is consisting of a constant 1 and a pair of spherical Bernstein–Bezier polynomials of the first order $g_1(\mathbf{r})$ and $g_2(\mathbf{r})$ is used.

Let $\mathbf{a}_1, \mathbf{a}_2, \mathbf{a}_3$ be the vectors pointing from the center of the sphere to the vertices of the triangle K_i . Then the basis functions are as following:

$$\begin{aligned}
 g_0(\mathbf{r}) &= 1, \\
 g_1(\mathbf{r}) &= \frac{(\mathbf{r}, \mathbf{a}_1, \mathbf{a}_2)}{(\mathbf{a}_1, \mathbf{a}_2, \mathbf{a}_3)}, \\
 g_2(\mathbf{r}) &= \frac{(\mathbf{r}, \mathbf{a}_2, \mathbf{a}_3)}{(\mathbf{a}_1, \mathbf{a}_2, \mathbf{a}_3)}.
 \end{aligned} \tag{1}$$

Also for brevity we use the notation:

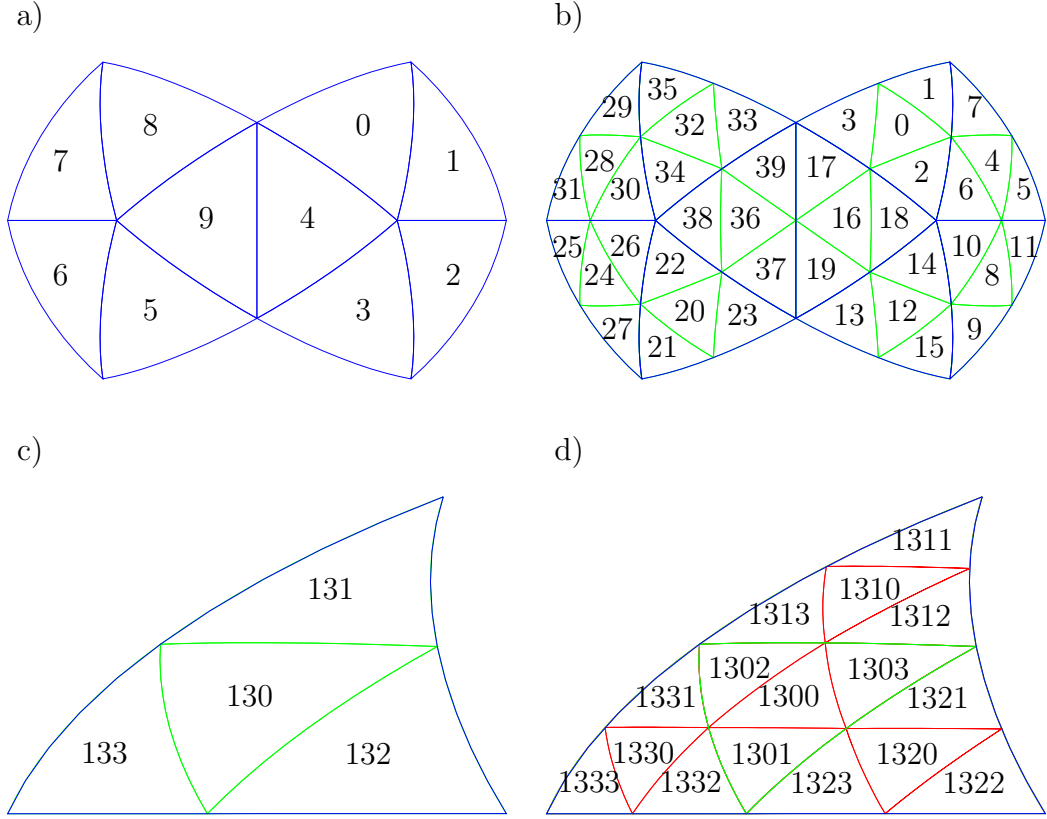


Figure 3: On figures (a) and (b) the decimal indices for two different decomposition steps are shown. On (a) there is no triangles decomposition, and on (b) one step is performed. Figures (c) and (d) represent indices for decompositions of triangle 7 from figure (a) in quaternary notation.

$$g_3 = \frac{(\mathbf{r}, \mathbf{a}_3, \mathbf{a}_1)}{(\mathbf{a}_1, \mathbf{a}_2, \mathbf{a}_3)}. \quad (2)$$

These first-order Bernstein–Bezier polynomials are in some sense the barycentric coordinates for the spherical triangles,

$$\mathbf{r} = g_1(\mathbf{r}) \mathbf{a}_3 + g_2(\mathbf{r}) \mathbf{a}_1 + g_3(\mathbf{r}) \mathbf{a}_2. \quad (3)$$

Also the axial part of gradients ∇_{\circ} of basis functions that utilized to construct the numerical method have a quite simple form:

$$\nabla_{\circ} g_1(\mathbf{r}) = \frac{[\mathbf{a}_1 \times \mathbf{a}_2]}{(\mathbf{a}_1, \mathbf{a}_2, \mathbf{a}_3)} - \mathbf{r} g_1(\mathbf{r}). \quad (4)$$

We omit the centering constants in the basis declaration. Those constants we subtract from g_1 and g_2 to made them orthogonal to g_0 in L_2 .

In the implementation of LDG method there are several integrals over cells and their boundaries we ought to compute. To calculate those integrals we first

project a spherical triangle to a plane one, and then use the known technique of the Gaussian quadrature for the plane triangle. We introduce the notation \mathcal{P}_i for the plane triangle constructed from the same vertices $\mathbf{a}_1, \mathbf{a}_2$ and \mathbf{a}_3 as the spherical one $K_i \in \mathcal{T}_h$. We get the following expression for the integral over the spherical triangle of some function $f(\mathbf{m})$:

$$\iint_{K_i} f(\mathbf{m}) d\mathbf{m} = \iint_{\mathcal{P}} f\left(\frac{\mathbf{r}}{|\mathbf{r}|}\right) \frac{(\mathbf{a}_1, \mathbf{a}_2, \mathbf{a}_3)}{|\mathbf{r}|^3} d\mathbf{r}. \quad (5)$$

The integration over the plane triangle \mathcal{P}_i is done using the four-point quadrature formula.

To calculate the integrals over the boundary of the spherical triangle the projection to the plane triangle is used too. The boundary ∂K_i consists of the three arcs $\widehat{\mathbf{a}_1, \mathbf{a}_2}$, $\widehat{\mathbf{a}_2, \mathbf{a}_3}$ and $\widehat{\mathbf{a}_3, \mathbf{a}_1}$. Consider the integral of the function $f(\mathbf{m})$ over the arc $\widehat{\mathbf{a}_1, \mathbf{a}_2}$. The straight line connecting the points is denoted by $\overline{\mathbf{a}_1, \mathbf{a}_2}$. Then the integral over the arc can be expressed in terms of the integral over the line:

$$\int_{\widehat{\mathbf{a}_1, \mathbf{a}_2}} f(\mathbf{m}) d\mathbf{m} = \int_{\overline{\mathbf{a}_1, \mathbf{a}_2}} f\left(\frac{\mathbf{r}}{|\mathbf{r}|}\right) \frac{|[\mathbf{a}_1 \times \mathbf{a}_2]|}{|\mathbf{r}|^2} d\mathbf{r}. \quad (6)$$

To compute the integrals in the boundaries we use the three-point Gauss-Legendre quadrature rule.

2 The setting of the problem

The superparamagnetic material is an ensemble of non-interacting monodomain ferromagnetic microparticles. At the temperature below the Curie temperature this systems behaves as a paramagnetic with a large susceptibility. Superparamagnetics possess a whole range of interesting properties, in particular superparamagnetics provide the phenomena of the stochastic resonance, i.e. a non-monotone dependence of the response on the temperature at a constant frequency of the external alternating field. To simulate superparamagnetic we use the Fokker-Planck equation which describes the evolution of the distribution of the magnetic momentum of the monodomain particle. This equation was introduced by Brown in 1963 [8]:

$$\frac{\partial f(\mathbf{m}, t)}{\partial t} + \alpha (\nabla_{\circ}, [\mathbf{m} \times \mathbf{H}^{\text{eff}}] f(\mathbf{m}, t)) = \gamma (\nabla_{\circ}, [\mathbf{m} \times [\mathbf{m} \times (\mathbf{H}^{\text{eff}} - T\nabla_{\circ})]]) f(\mathbf{m}, t), \quad (7)$$

where

$$\mathbf{H}^{\text{eff}} = \mathbf{H}_0 + \mathbf{A} \sin(\Omega t) + K \mathbf{a}_3 (\mathbf{a}_3, \mathbf{m})^3,$$

$f(\mathbf{m}, t)$ is the distribution function of the magnetic momentum of the sample particles depending on the direction \mathbf{m} and the time t , ∇_{\circ} denotes the axial part of the gradient, α is the speed of the precession, γ is the dissipation coefficient, \mathbf{H}_0 is the constant external field, \mathbf{A} is the amplitude of the periodic external magnetic field, K , \mathbf{a}_3 are correspondingly the coefficients and the directions of the cubic anisotropy and T is the temperature of the thermostat which contains the sample.

3 The numerical method

3.1 The space integration

To simplify the further calculations let us introduce the flux:

$$\begin{aligned} Q(f) &= f, \\ \mathbf{F}(f) &= \alpha [\mathbf{m} \times \mathbf{H}^{\text{eff}}] f - \gamma [\mathbf{m} \times [\mathbf{m} \times \mathbf{H}^{\text{eff}}]] f, \\ \mathbf{G} &= \gamma T [\mathbf{m} \times [\mathbf{m} \times \mathbf{q}]]. \end{aligned} \quad (8)$$

After the substitution of the fluxes in the equation (7) we rewrite the second-order equation as a system of the convection equations in the divergent form,

$$\begin{cases} \mathbf{q}(\mathbf{m}, t) = -\nabla_{\circ} Q(f), \\ \frac{\partial f(\mathbf{m}, t)}{\partial t} + (\nabla_{\circ} \cdot \mathbf{F}(f)) = (\nabla_{\circ} \cdot \mathbf{G}(\mathbf{q})). \end{cases} \quad (9)$$

We have obtained a system of four first-order equations which we solve using the discontinuous Galerkin method. We look for the solution (f_h, \mathbf{q}_h) given by a linear combination of the basis functions g_j in any of the cells of the mesh with the coefficients of the combination depending only on time. Thus into the cell K_i we look for the solution in the following form:

$$\begin{cases} f_h(\mathbf{m}, t) = \sum_{j=0}^2 f_j(t) g_j(\mathbf{m}), \\ \mathbf{q}_h(\mathbf{m}, t) = \sum_{j=0}^2 \mathbf{q}_j(t) g_j(\mathbf{m}). \end{cases} \quad (10)$$

Let us write down the semi-discrete Galerkin method for the equation (9) and a probe function $\nu_h(\mathbf{m})$ which is an arbitrary linear combination of the basis functions g_0, g_1, g_2 :

$$\left\{ \begin{array}{l} \iint_{K_i} \mathbf{q}_h \nu_h \, d\mathbf{m} = - \oint_{\partial K_i} Q(f_h) \mathbf{n} \nu_h \, d\Gamma + \iint_{K_i} Q(f_h) \nabla_{\circ} \nu_h \, d\mathbf{m}, \\ \frac{d}{dt} \iint_{K_i} f_h \nu_h \, d\mathbf{m} + \oint_{\partial K_i} (\mathbf{F}(f_h) - \mathbf{G}(\mathbf{q}_h)) \cdot \mathbf{n} \nu_h \, d\Gamma - \\ \iint_{K_i} (\mathbf{F}(f_h) - \mathbf{G}(\mathbf{q}_h)) \cdot \nabla_{\circ} \nu_h \, d\mathbf{m} = 0. \end{array} \right. \quad (11)$$

The index n takes values from 0 to 2. We used here the curvilinear version of Ostrogradsky–Gauss theorem to evolve the integrals. Without loss of generality the equation (11) can be substituted by a system in which the probe function v_h is substituted in turn by each of the basis functions g_0, g_1 and g_2 .

$$\left\{ \begin{array}{l} \sum_{j=0}^2 \mathbf{q}_j \iint_{K_i} g_j g_n \, d\mathbf{m} + \oint_{\partial K_i} Q(f_h) \mathbf{n} g_n \, d\Gamma - \iint_{K_i} Q(f_h) \nabla_{\circ} g_n \, d\mathbf{m} = 0, \\ \sum_{j=0}^2 \frac{df_j}{dt} \iint_{K_i} g_j g_n \, d\mathbf{m} + \oint_{\partial K_i} (\mathbf{F}(f_h) - \mathbf{G}(\mathbf{q}_h)) \cdot \mathbf{n} g_n \, d\Gamma - \\ \iint_{K_i} (\mathbf{F}(f_h) - \mathbf{G}(\mathbf{q}_h)) \cdot \nabla_{\circ} g_n \, d\mathbf{m} = 0. \end{array} \right. \quad (12)$$

The introduction of the \mathbf{q} variable does not require storage of additional data in each of the mesh cells and can be computed locally. This very property explains the origin of the name of the LDG methods family.

Generically on the boundaries of the cells the solution experiences discontinuity hence there is no unique way to calculate the flux through the boundary. This is a reason why we introduce the numerical fluxes.

3.2 The numerical fluxes

For the fluxes describing the convective part we use the notations introduced in [1] for the jump value and the average value of some function p on the cell's boundary:

$$\begin{aligned} [p] &= p^{\text{out}} - p^{\text{in}}, \\ \{p\} &= \frac{p^{\text{in}} + p^{\text{out}}}{2}. \end{aligned} \quad (13)$$

We substitute the flux $(\mathbf{F}(f_h) \cdot \mathbf{n})$ with the numerical Lax–Friedrichs flux $\hat{F}(f_h)$, defined by the formula:

$$\hat{\mathbf{F}}(f_h) = \{\mathbf{F}(f_h)\} \cdot \mathbf{n} - \frac{C}{2} [f_h], \quad (14)$$

where $C = \max_{f \in [f^{\text{in}}, f^{\text{out}}]} \left\{ \frac{\partial}{\partial f} \mathbf{F}(f) \cdot \mathbf{n} \right\}$ is the maximal characteristic speed.

To reach the optimal convergence order the fluxes for the diffusion terms should be substituted by the special numerical fluxes [11]. The calculation of these fluxes does not present a considerable complication but requires the introduction of a new entity: for each boundary we must define which of the adjoining cells is the right one. The other cell we call the left one.

To define the direction for every edge we choose the special axis \mathbf{o} connecting two mesh vertices on the sphere. We use two opposite vertices for additional symmetry. In each point of the quadrature formulae on the cell boundaries the direction of the vector product of the radius-vector of the point and the axis $\mathbf{l} = \mathbf{r} \times \mathbf{o}$ is computed. If the resulting vector \mathbf{l} points inside the cell then the cell is left, otherwise right.

It is certainly not the unique way to distinguish between left and right cells but it guarantees absence of the cells which have no right neighbours and which correspondingly are not accounted for in the calculation of the diffusion. The absence of the left neighbours also leads to the absence of the diffusion through the cell's boundary.

Having defined the left and right cells we finally can write down the numerical fluxes for the diffusion through their common boundary,

$$\begin{cases} \hat{Q}(f_h) \mathbf{n} & = f_h^R \mathbf{n}, \\ \hat{G}(\mathbf{q}_h) \cdot \mathbf{n} & = \mathbf{q}_h^L \cdot \mathbf{n}. \end{cases} \quad (15)$$

3.3 The time integration

Having substituted the quadrature formulae for the space integration into the equations (12) we arrive to the system which can be written in a compact form $\frac{d\xi}{dt} = L\xi$, where $\xi = (f_0, f_1, f_2, \mathbf{q}_0, \mathbf{q}_1, \mathbf{q}_2)$, and L is a certain operator, in our case linear. To integrate this ODE system over time we use the second-order TVD Runge–Kutta method, also known as Heun's method [12]. If we take time step to be equal to h , then the time integration looks as following:

$$\begin{cases} \xi^{(1)} = \xi^{(0)} + hL(\xi^{(0)}), \\ \xi^{(2)} = \frac{1}{2}\xi^{(1)} + \frac{1}{2}hL(\xi^{(1)}). \end{cases} \quad (16)$$

Since we use the explicit time integration the time step is subject to the CFL condition. In our case this condition is quadratic in space. Hence using of such approach is sensible only in the convection dominated problems. For all setups where we have the positive diffusion we can obtain the monotonicity of the scheme without introduction a limiter. For settings without the diffusion we used the WENO limiter introduced in the paper [3]. That completes the definition of the computational method.

4 The results of the simulations

For the Brown equation in absence of the periodic external field or anisotropy the stationary distribution is available which reads as (up to normalization factor):

$$f^*(\mathbf{m}) = \exp\left(\frac{\mathbf{m}\mathbf{H}}{T}\right). \quad (17)$$

By means of this function the coordinate momentum along the field can be calculated (without loss of generality assume that the field is directed along z axis),

$$\langle m_z \rangle = \text{cth}\left(\frac{|\mathbf{H}|}{T}\right) - \frac{T}{|\mathbf{H}|}. \quad (18)$$

Another setting to test the method is $T = 0$. In this setting the characteristics are available [7]:

$$\begin{cases} \varphi(h) = \varphi_0 - \alpha|\mathbf{H}_0|h, \\ \theta(h) = 2 \arctg\left(\text{tg} \frac{\theta_0}{2} \exp[-\gamma|\mathbf{H}_0|h]\right), \end{cases} \quad (19)$$

where φ and θ are the spherical coordinates and the θ angle is counted from the magnetic field direction.

We consider these two settings without anisotropy and in presence of the unit constant field to estimate the convergence.

1. At $T = 0.1, \gamma = 0.1, \alpha = 1$ and the stationary distribution is chosen as an initial distribution. The duration of the calculation is taken to be sufficient for the distribution to settle. In this case the duration is $\frac{3\pi}{2\gamma}$. In this setting we measured the deviation of the first momentum of the coordinate along the field $|\delta \langle z \rangle|$ in the stationary distribution from the theoretical values given by the formula (18).
2. At $\gamma = 0, \alpha = 1$ let us consider the error in calculation of oscillation frequency. This parameter is crucial for long-duration calculations because the phase error is accumulated due to the deviation of frequency. The duration of the calculation was taken to be no less than 50 periods. From the formula (19) the theoretical value of the oscillation frequency could be derived. It equals to α .

The figure 5 shows that the deviation of the second momentum decreases linearly when the number of the cells is increased. Taking into account the connection of the cell diameter with the number of cells (cf. fig. 2) we obtain the second order of accuracy for this quantity.

The results for the second setting are presented on the fig. 4. We see

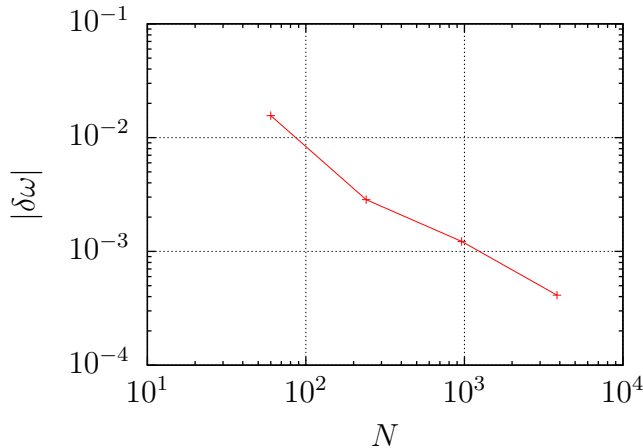


Figure 4: The dependence of frequency error $\delta\omega$ on the number of mesh cells N .

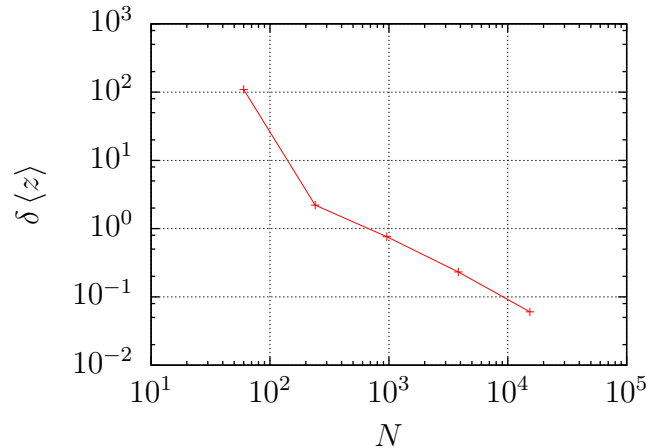


Figure 5: The dependence of the deviation of the first momentum along the field in the stationary distribution $\delta\langle z \rangle$ on the number of cells N at $\gamma = 0.1, T = 0.1, \alpha = 1$.

that the phase errors depend on the diameter of the tessellation as quadratic function and they are sufficiently small for long-duration calculations. As you can see there is no diffusion in this setting, therefore we were forced to use the WENO limiter. Nevertheless it does not sufficiently affect the phase errors.

We also simulate two anisotropic settings. The light axis type of anisotropy which was used in this work had its axis directed parallel to the external field. The direction of the periodical external field \mathbf{A} was perpendicular to the constant external field \mathbf{H} and its value was chosen to be 0.1. The first setup had value of external field $|\mathbf{H}|$ equals 2 that greater than the anisotropy constant K which value was chosen to be 1 in both settings. So in this setting we have one-well the unharmonic magnetostatic potential U defined by the following equation $\mathbf{H}^{\text{eff}} = -\nabla_{\mathbf{m}}U + \mathbf{A} \sin(\Omega t)$.

In the other setup the external field $|\mathbf{H}| = 0.5$ was lesser than anisotropy coefficient $K = 1$. Here we had double-well potential.

For both setups we calculated the response I on the periodical external field $\mathbf{A} \sin(\Omega t)$. We define the response as the amplitude of equilibrium oscillations in projection on the direction of periodical field and evaluate it according to the formula (20) as an amplitude of Fourier transformation of average mag-

netic moment projection on the direction of the driving force on it's frequency calculated on 40 periods of oscillations.

$$I = \frac{2\Omega}{|\mathbf{A}|80\pi} \left| \int_{\frac{5}{\gamma}}^{\frac{5}{\gamma} + \frac{80\pi}{\Omega}} \int_{\circ} \frac{(\mathbf{m} \cdot \mathbf{A})}{|\mathbf{A}|} f(\mathbf{m}, t) \, d\mathbf{m} e^{i\Omega t} \, dt \right| \quad (20)$$

Results for the first setting are represented on the fig. 6. On this figure we see that the paramagnetic resonance frequency decreasing if the system temperature increasing. The cause of this effect is that our system is unharmonic and therefore the period of precession depends on it's energy. By increasing the temperature of the system we enlarging the average energy of the system hence reducing it's frequency. The response dependence for the other setting displayed on the fig. 7. In this case $|\mathbf{H}| < K$ and magnetostatic potential become double-well potential. For each of potential wells we have fundamental frequency. So we can clearly see two maximums on fundamental frequencies for the each well.

On the both figures we can see nonmonotone dependence of response on the temperature.

Concluding remarks

The purpose of this work was the construction and the verification of the LDG method on the sphere on a recursive mesh consisting of spherical triangles. As an example for the simulation the Fokker–Planck equation was chosen which describes the evolution of the magnetic moment distribution for a superparamagnetic system. The accuracy of the method was proven by two variants of the setting which confirmed the convergence of the system to be of the second order. The value of the phase error proved to be sufficient for simulation of the resonance properties of the superparamagnetic materials. The frequency error of the implemented method appeared to be sensibly small therefore we can use this method for calculations of resonant phenomena. The response dependence on the frequency of driving force and the temperature for two systems with qualitatively different magnetostatic potentials was calculated. Stochastic resonance was observed in each case.

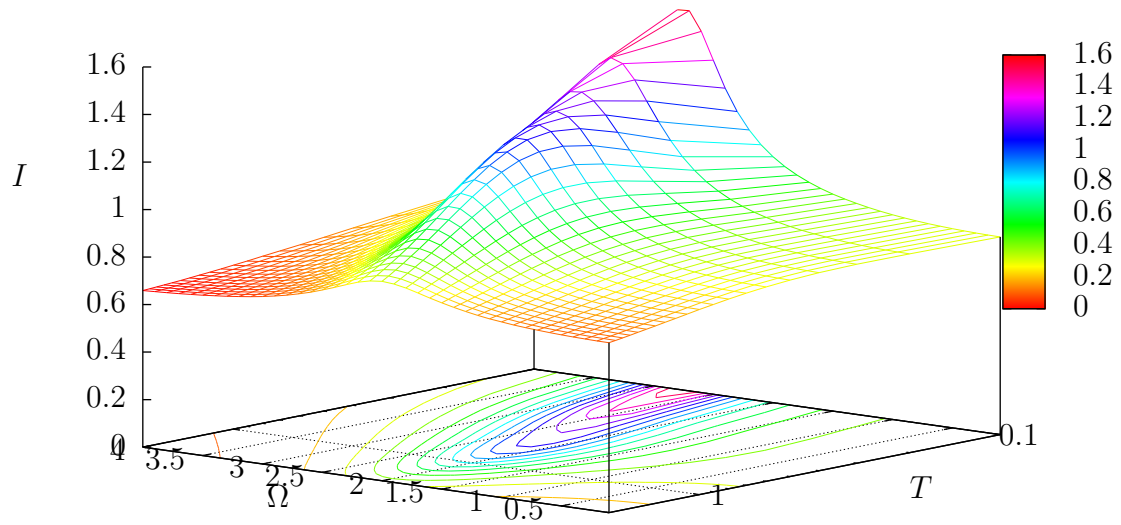


Figure 6: The dependence of the response on the frequency Ω and the temperature T for $2 = |\mathbf{H}| > K = 1$

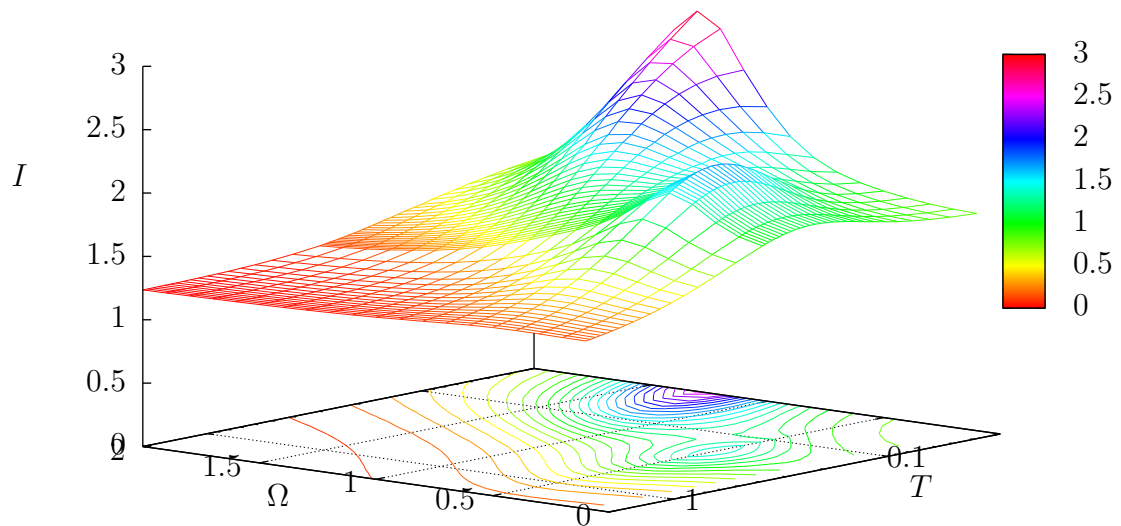


Figure 7: The dependence of the response on the frequency Ω and the temperature T for $0.5 = |\mathbf{H}| < K = 1$

References

- [1] Cockburn B, Shu C W, for Computer Applications in Science I and Engineering 2000 *Runge-Kutta discontinuous Galerkin methods for convection-dominated problems [microform]* / Bernardo Cockburn, Chi-Wang Shu (ICASE, NASA Langley Research Center ; Available from NASA Center for Aerospace Information Hampton, VA : Hanover, MD)
- [2] Georgoulis E H, Hall E and Houston P 2009 *Applied Numerical Mathematics* **59** 2179 – 2194 ISSN 0168-9274 second Chilean Workshop on Numerical Analysis of Partial Differential Equations (WONAPDE 2007)
- [3] Xu Z, Liu Y and Shu C W 2009 *Journal of Computational Physics* **228** 2194 – 2212 ISSN 0021-9991
- [4] Zhang X and Shu C W 2010 *Journal of Computational Physics* **229** 8918 – 8934 ISSN 0021-9991
- [5] Ronchi C, Iacono R and Paolucci P 1996 *Journal of Computational Physics* **124** 93 – 114 ISSN 0021-9991
- [6] Giraldo F, Hesthaven J and Warburton T 2002 *Journal of Computational Physics* **181** 499 – 525 ISSN 0021-9991
- [7] Ivanov A 2007 *Matem. Mod.* **19** 89–104
- [8] Brown W F 1963 *Phys. Rev.* **130**(5) 1677–1686
- [9] Morton A 1966 A computer oriented geodetic data base and a new technique in file sequencing Tech. rep. IBM Ltd., Ottawa, Ontario, Canada, 1966
- [10] Alfeld P, Neamtu M and Schumaker L L 1996 *Journal of Computational and Applied Mathematics* **73** 5 – 43 ISSN 0377-0427
- [11] Xu Y and Shu C W 2010 *Communication in computational physics* **7** 1 – 46 ISSN 1991-7120
- [12] Shu C W and Osher S 1988 *Journal of Computational Physics* **77** 439 – 471 ISSN 0021-9991